AAEC/E325

AAEC/E325

AUSTRALIAN ATOMIC ENERGY COMMISSION

RESEARCH ESTABLISHMENT

LUCAS HEIGHTS

THE EFFECT OF PRESSURE ON BURNOUT IN A ROUND TUBE COOLED BY FREON–12

by

V. ILIC

December 1974

ISBN 0 642 99665 2

AUSTRALIAN ATOMIC ENERGY COMMISSION
RESEARCH ESTABLISHMENT
LUCAS HEIGHTS

THE EFFECT OF PRESSURE ON BURNOUT IN A ROUND TUBE COOLED BY FREON-12

by

V. ILIC

ABSTRACT

A resistance heated, uniform wall thickness, stainless steel tube (16 mm i.d. x 2,860 mm long) with an upflow of Freon-12 (dichlorodifluoromethane), subcooled at the inlet, was used to obtain data of the effect of pressure on burnout heat flux. Values of reduced pressure (ratio of system pressure to the critical pressure of the fluid) at inlet to the test section were in the range 0.2 - 0.4, with mass velocity ranging 0.8 - 4.1 Mg $m^{-2}s^{-1}$.

Data are adequately described by an existing correlation, except at the lowest test pressure (reduced pressure of 0.215) where the experimental values of burnout heat flux were up to 40 per cent higher.

National Library of Australia card number and ISBN 0 642 99665 2

The following descriptors have been selected from the INIS Thesaurus to describe the subject content of this report for information retrieval purposes. For further details please refer to IAEA–INIS–12 (INIS: Manual for Indexing) and IAEA–INIS–13 (INIS: Thesaurus) published in Vienna by the International Atomic Energy Agency.

BURNOUT; CRITICAL HEAT FLUX; FLOW RATE; FREONS; PRESSURE DEPENDENCE; PRESSURE DROP; SUBCOOLING; TUBES

CONTENTS

		Page
1.	INTRODUCTION	1
2.	DESCRIPTION OF EXPERIMENT	1
	2.1 Test Section	1
	2.2 Instrumentation	1
	2.3 Method of Measurement	2
	2.4 Experimental Errors	2
3.	EXPERIMENTAL RESULTS	2
	3.1 General	2
	3.2 Observations and Discussion	3
4.	CONCLUSIONS	4
5.	RECOMMENDATIONS	4
6.	NOMENCLATURE	5
7.	ACKNOWLEDGEMENTS	5
8.	REFERENCES	5

Table 1 Burnout Data

Figure 1 General arrangement of the test section in the test loop

Figure 2 Variation of BHF with p_i for 0, 4.7, 14 and 23.3 kJ kg^{-1} inlet subcooling

Figure 3 Variation of BOP with p_i at 40°C inlet temperature for mass velocities 1, 2 and 3 Mg $m^{-2}s^{-1}$

Figure 4 BOP CISE correlation error histogram

1. INTRODUCTION

Data for the upper limit of heat transfer rate (burnout) are of particular interest for design and accident studies associated with water-cooled nuclear reactor systems. The main objective of this work was to provide experimental data on the variation of burnout heat flux (BHF) with test section inlet pressure (p_i), at various mass velocities (G) and values of inlet subcooling (Δh_i). The effect of pressure on burnout power for the simple tube geometry has been determined from measurements using Freon-12.

The data obtained, together with suitable water data, will enable investigations to be made into the generality of BHF scaling techniques initially developed for a single pressure (6.89 MPa in water); these are currently under review and development at the AAEC Research Establishment.

2. DESCRIPTION OF EXPERIMENT

Tests were carried out in the AAEC experimental Freon burnout rig, ACTOR (Ilic 1972), in which the test section was vertical and the flow of liquid Freon-12 was directed through the test section in an upward direction. The tube was resistance heated by d.c. current supplied by a 150 kVA voltage regulated power supply.

2.1 Test Section

The test section, shown in position in the rig in Figure 1, was a stainless steel tube made to the following specifications:

Material	stainless steel (AS-G19-321)
Length, mm (in)	2,860 (112.75)
Inside diameter, mm (in)	16.1(0.633)
Wall thickness, mm (in)	1.1(0.045)
Resistance at 20°C, ohm	0.0342
Average inside surface roughness of tube	0.5×10^{-3} mm (20×10^{-6} in)

2.2 Instrumentation

The flowrate of liquid Freon-12 was measured by using an orifice plate. The test section power was obtained from separate measurements of applied voltage across the tube, and voltage across precision resistance shunts. These measurements were read off a digital voltmeter, as was the potential drop across a platinum resistance thermometer used for inlet temperature measurements. The temperature of the metered flow was measured with a chromel-alumel thermocouple located 2 m upstream of the orifice plate, and read off a temperature recorder chart.

The burnout indicator was a bridge device, similar to that described by Salt & Wintle (1964); a change in resistance in one half of the test section would cause an e.m.f. unbalance across a galvanometer, giving rise to the burnout alarm signal. This was always confirmed by a thermocouple attached to the test section wall at the outlet and in close thermal contact with it. Both signals were monitored by a pen recorder.

The system pressure was measured at the test section inlet (Figure 1) with a pressure transmitter and it was read off an indicator mounted in the instrument console.

A 1.5 m mercury manometer was used for measurement of test section pressure drop. The values of pressure drop presented in Table 1 have been corrected for the gravitational head corresponding to the unheated length from the upstream pressure tapping to the start of the heated length.

2.3 Method of Measurement

Trial burnout was reached by successive increments of power to the test section, at suitable time intervals. Test section voltage was then reduced by about 0.5 V, flow conditions were allowed to settle, and then burnout was again obtained. For a given pressure at the test section inlet, this was repeated for different inlet temperatures and mass flowrates.

2.4 Experimental Errors

The estimates of experimental errors are as follows:

flowrate	± 1.3%	power	± 1.3%
inlet pressure	± 14 kPa	test section heated area	± 0.6%
inlet temperature	± 1°C	test section pressure drop	± 1.0%

3. EXPERIMENTAL RESULTS

3.1 General

Burnout data recorded in the experiments were processed on an IBM360/50 computer using a specially developed computer program FREON (M.A. Cowper, AAEC unpublished report). These data are tabulated in Table 1.

Exit quality and boiling length were obtained from a heat balance calculation, neglecting losses to the surrounding air from the test section and copper power clamps. This is probably the reason that the quality exceeds 1 at low mass velocity.

The BHF data were taken over the following ranges of parameters:

inlet pressure	MPa (psia)	0.89(128) - 1.60(232)
mass velocity	Mg $m^{-2}s^{-1}$ (10^6 lb $ft^{-2}h^{-1}$)	0.81(0.6) - 4.07(3.0)
inlet subcooling	kJ kg^{-1}(Btu lb^{-1})	0.23(1.0) - 23.3(10.0)

These data are presented in Table 1 and the salient features are shown in graphical form in Figures 2 and 3.

3.2 Observations and Discussion

The data are presented graphically in terms of burnout heat flux variation with inlet pressure for four arbitrarily chosen values of inlet subcooling (0, 4.7, 14.0 and 23.3 kJ kg^{-1}) for a range of mass velocities (Figure 2). To obtain the variation of burnout heat flux with inlet pressure, a series of cross plots had to be made.

First, for a given inlet pressure, experimental data were plotted in terms of burnout heat flux against inlet subcooling, the relationship, in general, being linear for a given mass velocity. Then, for an arbitrarily selected set of values of inlet subcooling, the corresponding values of burnout heat flux were obtained for each mass velocity used in the tests. In particular, the data for the saturation inlet conditions were obtained by linear extrapolation to $\Delta h_i=0$. This enabled burnout heat flux *versus* mass velocity plots to be made for each selected value of inlet subcooling for the four inlet pressures. It was then possible to obtain values of burnout heat flux for chosen values of mass velocity at a given value of inlet subcooling and inlet pressure, such that the direct variation of burnout heat flux with pressure could be plotted (Figure 2).

In general, burnout heat flux is a strong function of the system pressure (Figure 2) for a range of values of mass velocity and four values of inlet subcooling. The highest value of burnout heat flux seems to occur at the least value of inlet pressure. Increasing the inlet pressure generally decreases the burnout heat flux for a given mass velocity and inlet subcooling. Increasing either the mass velocity, the inlet subcooling, or both enhances the burnout heat flux. It is interesting to observe that if the inlet temperature is kept constant, the burnout power may increase with increase of the inlet pressure over much of the pressure range (Figure 3). This is qualitatively consistent with Collier's (1972) observations for water.

A representative sample of data was compared with predicted values using the CISE burnout correlation adjusted for the effect of inlet pressure (Cumo

Ferrari & Urbani 1972):

$$W = \frac{A}{1+B} \cdot C \cdot E \quad ,$$

where $$A = \frac{1-R}{\left(\frac{G}{10^3}\right)^{1/3}} + \frac{\Delta h_i}{\lambda_i} \quad ,$$

$$B = 378.5738\, D^{1.4} \left(\frac{1}{R-1}\right)^{0.4} \frac{G}{10^3} \cdot \frac{1}{L} \quad ,$$

$$C = 0.7853976\, GD^2 \lambda_i \quad \text{and}$$

$$E = 1 - \frac{\frac{1}{4}-R}{\left(\frac{9}{4}-R\right)^2} \quad \text{for } R \geqslant 0.25 \quad .$$

The distribution of error, defined as $\frac{W-W_E}{W_E} \times 100$ is shown in Figure 4. It is apparent that most (73.5 per cent) of the data fall within ± 10 per cent of the predicted values. Data showing maximum deviation are at the least value of inlet pressure (0.89 MPa or reduced pressure of 0.215), which is below the pressure range for which the burnout correlation is suitable.

4. CONCLUSIONS

(i) Over the range of inlet static pressures used (reduced pressures of 0.215 to 0.390), the burnout heat flux usually decreased with increase in pressure for constant values of inlet subcooling and mass velocity. The variation of the burnout heat flux with pressure is non-linear and is not a simple one; it depends to some extent on mass velocity and inlet subcooling.

(ii) Comparison with a recent version of the CISE burnout correlation shows that 74 per cent of the data fall within ± 10 per cent of the predicted values. The only substantial deviations (> 12 per cent) were for the least value of the inlet pressure which is below the minimum pressure for which the correlation was developed.

5. RECOMMENDATIONS

(i) As a logical extension of the burnout data investigation with a tube, similar experiments ought to be carried out, with test sections of more complex geometry, to ascertain the suitability of the CISE or a similar burnout correlation.

(ii) It would be interesting and, perhaps conducive to a better understanding of the burnout phenomenon, to investigate in more detail the effect

of pressure on burnout in the region of high mass velocity and subcooling.

6. NOMENCLATURE

(i) Roman letters

D - hydraulic diameter

G - mass velocity

h - enthalpy

L - heated length

p - pressure

R - reduced pressure = $\frac{p}{p_c}$

t - temperature

W - burnout power

(ii) Greek letters

Δ - a small portion

λ - latent heat of vaporisation

(iii) Subscripts

B - boiling

BO - burnout

c - at the critical point

E - experimental

i - inlet

(iv) Abbreviations

BHF - burnout heat flux

BOP - burnout power

7. ACKNOWLEDGEMENTS

The author is grateful to the many people who assisted him in this project. In particular, the author thanks Dr. K.R. Lawther, Head, Heat Transfer Section, for his critical comments on a draft of this report, and Messrs. H.N. Harvey, J.R. Stevens and Miss A. Beard for their able technical assistance.

8. REFERENCES

Collier, J.G. (1972) - Convective Boiling and Condensation. McGraw Hill, London.

Cumo, M., Ferrari, G. & Urbani, G. (1972) - Prediction of Burnout Power with Freon up to the Critical Pressure. Advances in Heat Transfer RT/ING(72)19, Comitato Nazionale Energie Nucleare.

Ilic, V. (1972) - The AAEC Freon Burnout Rig ACTOR and Initial Boiling Crisis (Burnout) Results. AAEC/TM632.

Salt, K.J. & Wintle, C.A. (1964) - Design and Operation of a Transistorised Bridge Type Detector for Burnout in Boiling Heat Transfer Experiments. AEEW-R330.

TABLE 1

BURNOUT DATA

Test Section	type material mode of heating heater length mm (in) heater resistance (at 20C) ohm distance between pressure taps mm (in)	tube stainless steel AS-G19-321 d.c. resistance heating 2860 (112.75) 0.0342 3200 (126.00)
Geometry	internal diameter mm (in) wall thickness mm (in) surface roughness mm (in)	16.1 (0.633) 1.1 (0.045) 0.5×10^{-3} (20×10^{-6})
Burnout detector	resistance type	

Run number	Inlet Pressure		Inlet Subcooling		Mass Velocity		Burnout Flux		Exit Quality	Power kW	Test Section Pressure Drop				Boiling Length	
											Zero Power		With Power			
	MPa	psia	kJ kg^{-1}	Btu lb^{-1}	kg $s^{-1} m^{-2}$ $\times 10^{-3}$	lb $h^{-1} ft^{-2}$ $\times 10^{-6}$	kW m^{-2}	Btu $h^{-1} ft^{-2}$ $\times 10^{-4}$			kPa	psi	kPa	psi	m	ft
22087012	1.064	154.36	14.05	6.04	0.203	0.150	42.3	1.34	1.065	6.12	37.3	5.41	12.91	1.873	2.591	8.5
22087010	1.064	154.36	14.05	6.04	0.203	0.150	41.7	1.32	1.049	6.03	37.3	5.41	13.18	1.912	2.588	8.49
23087002	1.061	153.85	8.12	3.49	0.203	0.150	39.1	1.24	1.021	5.66	36.34	5.27	12.13	1.76	2.694	8.84
22087019	1.061	153.85	8.16	3.51	0.205	0.151	39.5	1.25	1.026	5.71	36.34	5.27	9.087	1.318	2.694	8.84
22087017	1.061	153.85	8.16	3.51	0.205	0.151	38.5	1.22	0.999	5.57	36.34	5.27	9.087	1.318	2.688	8.82
22087008	1.064	154.36	23.61	10.15	0.205	0.151	44.0	1.40	1.027	6.37	-	-	14.53	2.107	2.42	7.94
22087006	1.064	154.36	23.61	10.15	0.205	0.151	44.0	1.39	1.025	6.36	-	-	14.62	2.12	2.42	7.94
28087034	0.887	128.60	20.75	8.92	0.647	0.477	99.0	3.14	0.678	14.32	39.16	5.68	27.09	3.929	2.320	7.61
28087042	0.887	128.60	13.28	5.71	0.648	0.478	92.1	2.92	0.677	13.34	38.61	5.6	25.66	3.721	2.487	8.16
28087040	0.887	128.60	13.47	5.79	0.648	0.478	92.5	2.93	0.678	13.38	38.61	5.6	25.53	3.703	2.484	8.15
28087032	0.887	128.60	20.17	8.67	0.649	0.478	96.9	3.07	0.664	14.02	39.23	5.69	27.1	3.93	2.323	7.62
28087048	0.887	128.60	2.81	1.21	0.651	0.480	83.0	2.63	0.677	12.01	37.37	5.42	23.81	3.454	2.774	9.1
28087050	0.887	128.60	2.84	1.22	0.651	0.480	82.7	2.62	0.674	11.97	37.37	5.42	23.93	3.471	2.774	9.1
28087007	1.339	194.25	24.18	10.36	0.652	0.480	85.8	2.72	0.595	12.42	37.3	5.41	23.33	3.383	2.128	6.98
28087009	1.339	194.25	24.00	10.32	0.652	0.480	85.5	2.71	0.593	12.37	37.3	5.41	23.64	3.428	2.128	6.98
28087025	1.339	194.25	5.98	2.57	0.652	0.481	70.2	2.23	0.603	10.16	35.09	5.09	20.37	2.955	2.640	8.66
28087017	1.339	194.25	15.26	6.56	0.652	0.481	79.1	2.51	0.606	11.44	36.2	5.25	21.92	3.179	2.359	7.74
28087015	1.339	194.25	15.24	6.55	0.652	0.481	78.8	2.50	0.604	11.4	36.2	5.25	21.62	3.135	2.356	7.73
28087023	1.339	194.25	5.47	2.35	0.653	0.481	70.5	2.24	0.609	10.21	35.16	5.1	20.23	2.934	2.661	8.73
27087021	1.604	232.63	21.70	9.33	0.657	0.484	75.8	2.40	0.548	10.97	36.27	5.26	23.63	3.427	2.109	6.92
27087027	1.604	232.63	14.89	6.4	0.657	0.485	69.0	2.19	0.542	9.98	35.16	5.1	22.23	3.224	2.292	7.52
27087029	1.604	232.63	14.79	6.36	0.657	0.485	68.8	2.18	0.541	9.96	35.16	5.1	22.05	3.198	2.295	7.53

Run Number	Inlet Pressure		Inlet Subcooling		Mass Velocity		Burnout Flux		Exit Quality	Power kW	Test Section Pressure Drop				Boiling Length	
											Zero Power		With Power			
	MPa	psia	kJ kg^{-1}	Btu lb^{-1}	kg s^{-1} m^{-2} x 10^{-3}	lb h^{-1} ft^{-2} x 10^{-6}	kW m^{-2}	Btu $h^{-1}ft^{-2}$ x 10^{-4}			kPa	psi	kPa	psi	m	ft
27087019	1.604	232.63	21.80	9.37	0.658	0.484	75.0	2.38	0.538	10.85	36.27	5.26	20.28	2.942	2.097	6.88
27087037	1.604	232.63	4.65	2.0	0.658	0.485	60.6	1.92	0.551	8.76	34.06	4.94	19.64	2.848	2.661	8.73
27087035	1.604	232.63	4.54	1.95	0.658	0.485	61.5	1.95	0.561	8.9	34.06	4.94	19.58	2.84	2.670	8.76
21087016	1.064	154.36	25.38	10.91	1.035	0.763	112.0	3.55	0.420	16.22	-	-	34.12	4.949	1.923	6.31
21087014	1.064	154.36	25.38	10.91	1.035	0.763	112.8	3.58	0.424	16.32	-	-	34.12	4.949	1.929	6.33
21087018	1.064	154.36	14.17	6.09	1.037	0.765	103.3	3.27	0.459	14.93	-	-	31.68	4.595	2.292	7.52
21087020	1.064	154.36	13.79	5.93	1.037	0.765	100.7	3.19	0.448	14.57	-	-	31.98	4.639	2.292	7.52
22087002	1.064	154.36	5.70	2.45	1.037	0.765	90.7	2.87	0.457	13.11	-	-	31.03	4.500	2.603	8.54
22087004	1.064	154.36	5.65	2.43	1.037	0.765	91.7	2.91	0.463	13.26	-	-	30.72	4.456	2.606	8.55
24087012	1.339	194.25	24.03	10.33	1.357	1.001	110.5	3.50	0.296	15.98	36.27	5.26	34.28	4.972	1.676	5.50
24087014	1.339	194.25	24.07	10.35	1.358	1.001	109.5	3.47	0.291	15.84	36.27	5.26	34.28	4.972	1.664	5.46
24087020	1.339	194.25	15.17	6.52	1.360	1.003	98.0	3.10	0.315	14.18	38.68	5.61	33.33	4.834	2.018	6.62
24087023	1.339	194.25	15.61	6.71	1.361	1.004	99.9	3.17	0.319	14.45	38.68	5.61	33.78	4.899	2.009	6.59
24087032	1.339	194.25	6.84	2.94	1.363	1.005	89.2	2.83	0.345	12.91	37.71	5.47	32.07	4.652	2.444	8.02
24087030	1.339	194.25	7.07	3.04	1.363	1.005	89.4	2.83	0.343	12.93	37.71	5.47	32.07	4.651	2.429	7.97
28087060	0.887	128.60	22.07	9.49	1.365	1.006	128.6	4.08	0.357	18.60	41.64	6.04	44.83	6.503	1.923	6.31
29087009	0.887	128.60	12.21	5.25	1.365	1.007	118.9	3.77	0.392	17.20	40.61	5.89	44.23	6.415	2.301	7.55
28087058	0.887	128.60	22.17	9.53	1.365	1.007	129.9	4.12	0.361	18.80	41.64	6.04	44.86	6.507	1.926	6.32
29087007	0.887	128.60	12.28	5.28	1.366	1.007	117.9	3.74	0.388	17.05	40.54	5.88	44.53	6.458	2.292	7.52
29087018	0.887	128.60	3.54	1.52	1.367	1.008	108.4	3.43	0.316	15.68	39.44	5.72	44.33	6.430	2.685	8.81
29087016	0.887	128.60	3.54	1.52	1.367	1.008	106.9	3.39	0.410	15.47	39.44	5.72	44.33	6.430	2.682	8.80
25087043	1.604	232.63	23.14	9.95	1.367	1.008	104.8	3.32	0.291	15.17	38.68	5.61	34.23	4.964	1.649	5.41
25087041	1.604	232.63	23.45	10.08	1.367	1.008	105.7	3.35	0.292	15.29	38.68	5.61	34.28	4.972	1.643	5.39
25087051	1.604	232.63	13.70	5.89	1.369	1.009	93.0	2.95	0.319	13.46	37.37	5.42	30.70	4.453	2.054	6.74
26087005	1.604	232.63	5.19	2.23	1.370	1.010	79.6	2.52	0.332	11.52	36.20	5.25	29.49	4.277	2.505	8.22
25087049	1.604	232.63	13.98	6.01	1.370	1.010	92.7	2.94	0.314	13.41	37.37	5.42	31.07	4.506	2.033	6.67
26087003	1.604	232.63	5.00	2.15	1.370	1.010	80.3	2.54	0.337	11.61	36.20	5.25	28.88	4.189	2.521	8.27

Run Number	Inlet Pressure		Inlet Subcooling		Mass Velocity		Burnout Flux		Exit Quality	Power kW	Test Section Pressure Drop				Boiling Length	
											Zero Power		With Power			
	MPa	psia	$kJ\ kg^{-1}$	$Btu\ lb^{-1}$	$kg\ s^{-1}\ m^{-2} \times 10^{-3}$	$lb\ h^{-1}\ ft^{-2} \times 10^{-6}$	$kW\ m^{-2}$	$Btu\ h^{-1} ft^{-2} \times 10^{-4}$			kPa	psi	kPa	psi	m	ft
21087004	1.064	154.36	23.68	10.18	2.125	1.567	133.7	4.23	0.183	19.34	43.37	6.29	48.32	7.008	1.35	4.43
21087002	1.064	154.36	23.77	10.22	2.125	1.567	133.0	4.21	0.180	19.23	43.37	6.29	48.14	6.982	1.338	4.39
21087008	1.064	154.36	14.68	6.31	2.126	1.567	122.9	3.89	0.225	17.77	-	-	48.70	7.064	1.844	6.05
21087006	1.064	154.36	14.75	6.34	2.126	1.567	122.5	3.88	0.224	17.72	-	-	49.16	7.130	1.835	6.02
21087010	1.064	154.36	6.23	2.68	2.126	1.567	112.3	3.56	0.264	16.25	-	-	49.73	7.212	2.39	7.84
21087012	1.064	154.36	6.33	2.72	2.126	1.567	112.8	3.57	0.264	16.31	-	-	49.73	7.212	2.384	7.82
19087009	1.064	154.36	16.05	6.90	2.126	1.567	123.8	3.92	0.217	17.90	42.47	6.16	49.06	7.115	1.756	5.76
19087013	1.064	154.36	16.19	6.96	2.127	1.568	124.0	3.93	0.216	17.94	42.47	6.16	48.93	7.097	7.747	5.73
20087015	1.064	154.36	24.31	10.45	2.129	1.569	133.3	4.23	0.176	19.28	43.37	6.29	48.25	6.998	1.305	4.28
20087022	1.064	154.36	6.77	2.91	2.131	1.571	112.2	3.56	0.259	16.24	41.37	6.00	49.57	7.189	2.347	7.70
25087034	1.339	194.25	5.84	2.51	4.111	3.031	114.3	3.62	0.144	16.53	53.99	7.83	89.89	13.037	2.018	6.62
25087033	1.339	194.25	5.84	2.51	4.111	3.031	116.1	3.68	0.145	16.79	53.99	7.83	83.80	12.154	2.033	6.67
25087024	1.339	194.25	15.19	6.53	4.111	3.031	120.8	3.83	0.070	17.48	55.09	7.99	68.47	9.930	0.786	2.58
27087013	1.604	232.63	10.65	4.58	4.114	3.033	114.8	3.64	0.102	16.61	52.81	7.66	69.71	10.111	1.329	4.36
27087011	1.604	232.63	10.72	4.61	4.113	3.033	112.9	3.58	0.098	16.34	52.81	7.66	70.17	10.177	1.295	4.25
25087026	1.339	194.25	15.33	6.59	4.116	3.035	119.5	3.79	0.067	17.30	55.09	7.99	69.07	10.018	0.744	2.44
27087004	1.604	232.63	15.00	6.45	4.117	3.036	119.5	3.79	0.068	17.29	53.37	7.74	63.11	9.154	0.783	2.57
27087002	1.604	232.63	14.58	6.27	4.117	3.036	119.8	3.80	0.072	17.33	53.37	7.74	60.08	8.714	0.847	2.78
30087019	0.887	128.60	12.16	5.23	4.117	3.036	144.2	4.57	0.132	20.86	58.19	8.44	103.55	15.018	1.466	4.81
30087026	0.887	128.60	3.05	1.31	4.117	3.036	144.8	4.59	0.211	20.95	57.09	8.28	135.30	19.623	2.515	8.25
25087014	1.339	194.25	23.84	10.25	4.117	3.036	147.5	4.68	0.035	21.34	55.85	8.10	65.31	9.472	0.189	0.62
30087017	0.887	128.60	12.12	5.21	4.118	3.037	142.4	4.51	0.130	20.60	58.19	8.44	103.46	15.005	1.457	4.78
26087043	1.604	232.63	21.72	9.34	4.119	3.037	141.1	4.47	0.042	20.42	54.54	7.91	63.14	9.158	0.314	1.03
26087041	1.604	232.63	21.70	9.33	4.119	3.037	140.7	4.46	0.041	20.35	54.54	7.91	62.87	9.119	0.308	1.01
30087010	0.887	128.60	21.38	9.19	4.120	3.038	151.1	4.79	0.065	21.86	57.99	8.41	80.77	11.715	0.521	1.71
30087008	0.887	128.60	21.42	9.21	4.121	3.038	153.0	4.85	0.067	22.13	57.99	8.41	81.38	11.803	0.546	1.79

Run Number	Inlet Pressure		Inlet Subcooling		Mass Velocity		Burnout Flux		Exit Quality	Power kW	Test Section Pressure Drop				Boiling Length	
											Zero Power		With Power			
	MPa	psia	$kJ\ kg^{-1}$	$Btu\ lb^{-1}$	$kg\ s^{-1}\ m^{-2} \times 10^{-3}$	$lb\ h^{-1}\ ft^{-2} \times 10^{-6}$	$kW\ m^{-2}$	$Btu\ h^{-1} ft^{-2} \times 10^{-4}$			kPa	psi	kPa	psi	m	ft
29087041	0.887	128.60	11.98	5.15	2.702	1.993	140.6	4.46	0.213	20.35	46.06	6.68	67.96	9.856	1.939	6.36
29087046	0.887	128.60	3.58	1.54	2.703	1.993	129.8	4.11	0.257	18.77	45.23	6.56	74.75	10.842	2.563	8.41
29087048	0.887	128.60	3.54	1.52	2.703	1.993	129.1	4.09	0.256	18.67	45.23	6.56	76.58	11.107	2.566	8.42
2908703	0.887	128.60	11.77	5.06	2.703	1.993	139.5	4.42	0.212	20.18	46.06	6.68	68.27	9.901	1.948	6.39
29087031	0.887	128.60	21.35	9.18	2.705	1.994	148.0	4.69	0.154	21.41	46.68	6.77	59.02	8.560	1.295	4.25
29087029	0.877	128.60	21.58	9.28	2.706	1.995	147.2	4.67	0.151	21.30	46.68	6.77	60.39	8.759	1.271	4.17
24087050	1.339	194.25	16.54	7.11	2.707	1.996	114.7	3.64	0.131	16.59	44.40	6.44	51.41	7.457	1.295	4.25
24087048	1.339	194.25	16.40	7.05	2.708	1.997	114.5	3.63	0.131	16.57	44.40	6.44	51.41	7.457	1.305	4.28
24087041	1.339	194.25	22.42	9.64	2.708	1.997	121.9	3.87	0.097	17.64	45.44	6.59	50.36	7.304	0.863	2.83
24087039	1.339	194.25	22.49	9.67	2.708	1.997	121.9	3.87	0.096	17.64	45.44	6.59	50.42	7.313	0.856	2.81
25087006	1.339	194.25	6.35	2.73	2.710	1.998	108.5	3.44	0.202	15.69	43.44	6.30	53.68	7.785	2.228	7.31
25087004	1.339	194.25	6.23	2.68	2.710	1.998	108.6	3.44	0.204	15.71	43.44	6.30	53.68	7.786	2.237	7.34
26087033	1.604	232.63	4.84	2.08	2.711	1.999	102.0	3.23	0.209	14.75	42.54	6.17	46.83	6.792	2.347	7.70
26087031	1.604	232.63	5.09	2.19	2.712	2.000	103.6	3.29	0.210	14.99	42.54	6.17	45.61	6.615	2.329	7.64
29087026	0.887	128.60	21.35	9.18	2.712	2.000	149.7	4.75	0.158	21.66	46.68	6.77	62.37	9.046	1.308	4.29
26087024	1.604	232.63	15.19	6.53	2.717	2.003	104.4	3.31	0.122	15.11	43.37	6.29	47.60	6.904	1.274	4.18
26087022	1.604	232.63	14.89	6.40	2.717	2.003	103.6	3.28	0.123	14.99	43.37	6.29	47.30	6.860	1.295	4.25
26087015	1.604	232.63	21.82	9.38	2.718	2.004	113.2	3.59	0.084	16.38	44.20	6.41	47.97	6.957	0.759	2.49
26087013	1.604	232.63	21.86	9.40	2.718	2.004	114.7	3.63	0.086	16.59	44.20	6.41	47.81	6.934	0.780	2.56
23087034	1.061	153.85	7.91	3.40	4.091	3.016	125.7	3.98	0.142	18.18	55.16	8.00	96.40	13.982	1.832	6.01
23087029	1.061	153.85	8.00	3.44	4.091	3.016	125.8	3.99	0.139	18.20	55.16	8.00	90.92	13.187	1.820	5.97
23087022	1.061	153.85	14.84	6.38	4.095	3.019	129.8	4.11	0.087	18.78	56.12	8.14	76.69	11.123	0.981	3.22
23087024	1.061	153.85	15.21	6.54	4.095	3.020	129.0	4.09	0.083	18.67	56.12	8.14	76.23	11.056	0.920	3.02
23087015	1.061	153.85	21.10	9.07	4.095	3.020	140.8	4.46	0.051	20.37	56.05	8.13	69.47	10.075	0.399	1.31
23087013	1.061	153.85	20.89	8.98	4.095	3.020	140.6	4.46	0.054	20.34	56.05	8.13	75.24	10.913	0.418	1.37
25087016	1.339	194.25	23.82	10.24	4.106	3.028	150.6	4.77	0.040	21.79	55.85	8.10	65.00	9.428	0.256	0.84

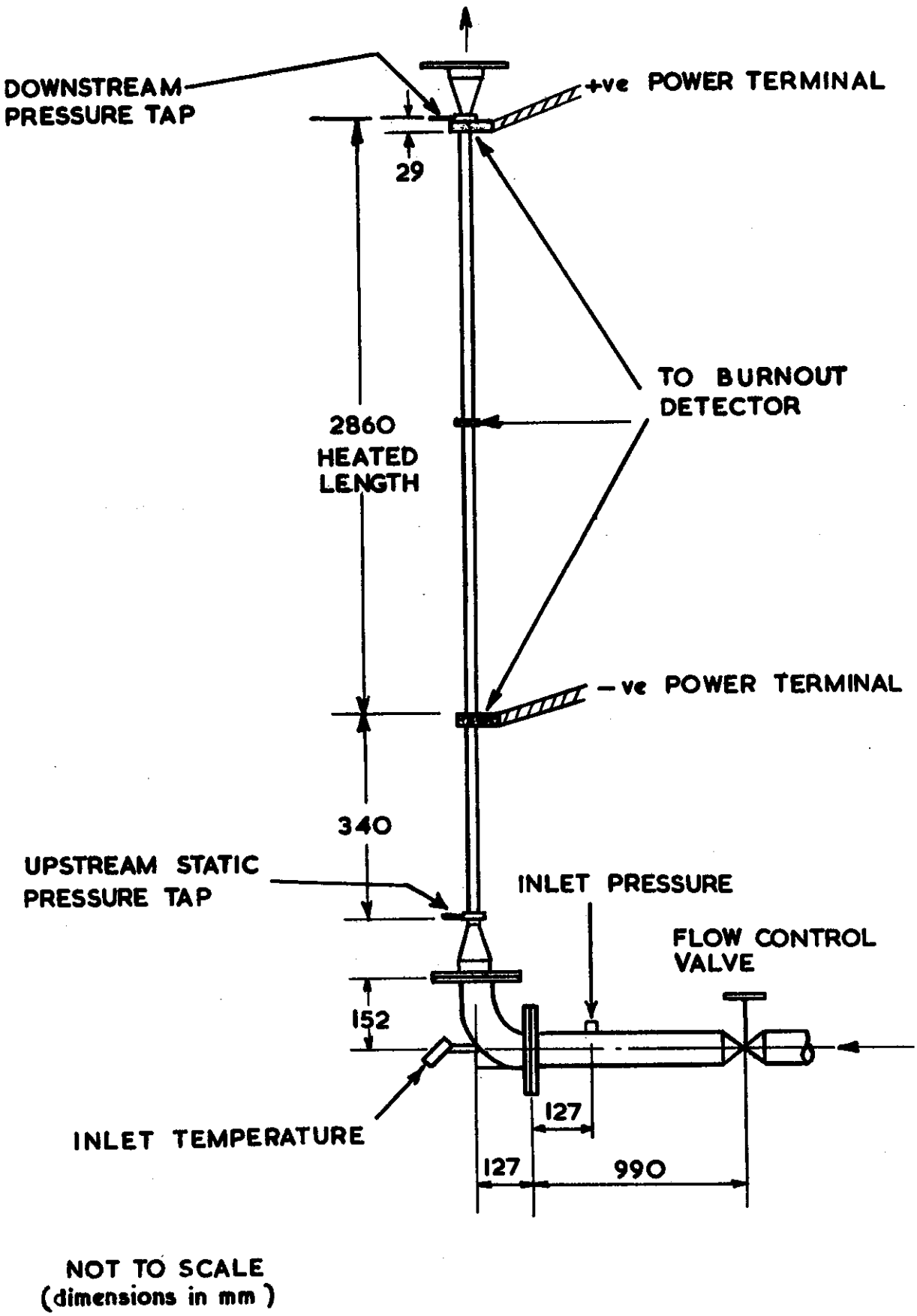

FIGURE 1. GENERAL ARRANGEMENT OF THE TEST SECTION IN THE TEST LOOP

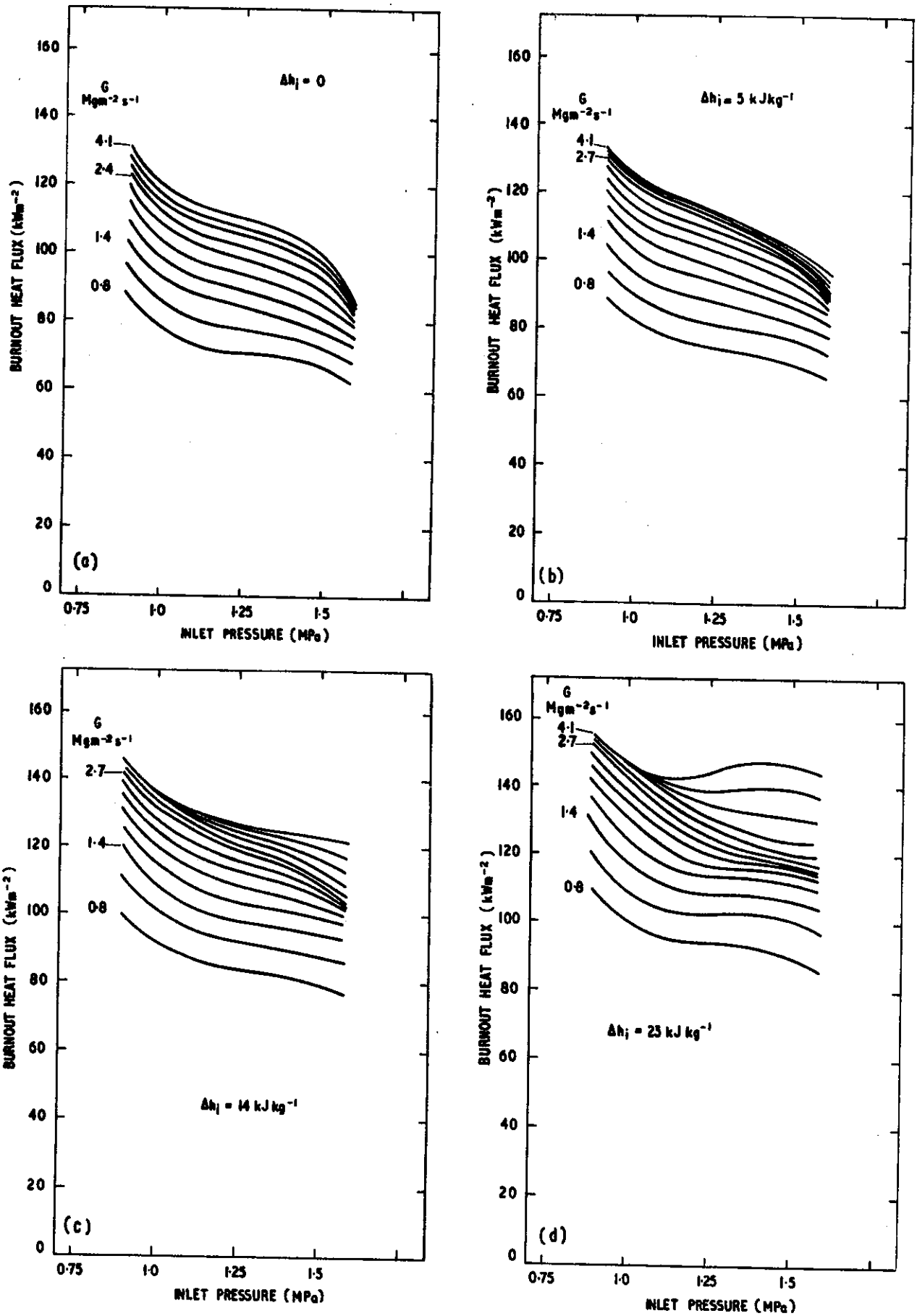

FIGURE 2. VARIATION OF BHF WITH p_i FOR 0, 4.7, 14 AND 23.3 kJ kg^{-1} INLET SUBCOOLING

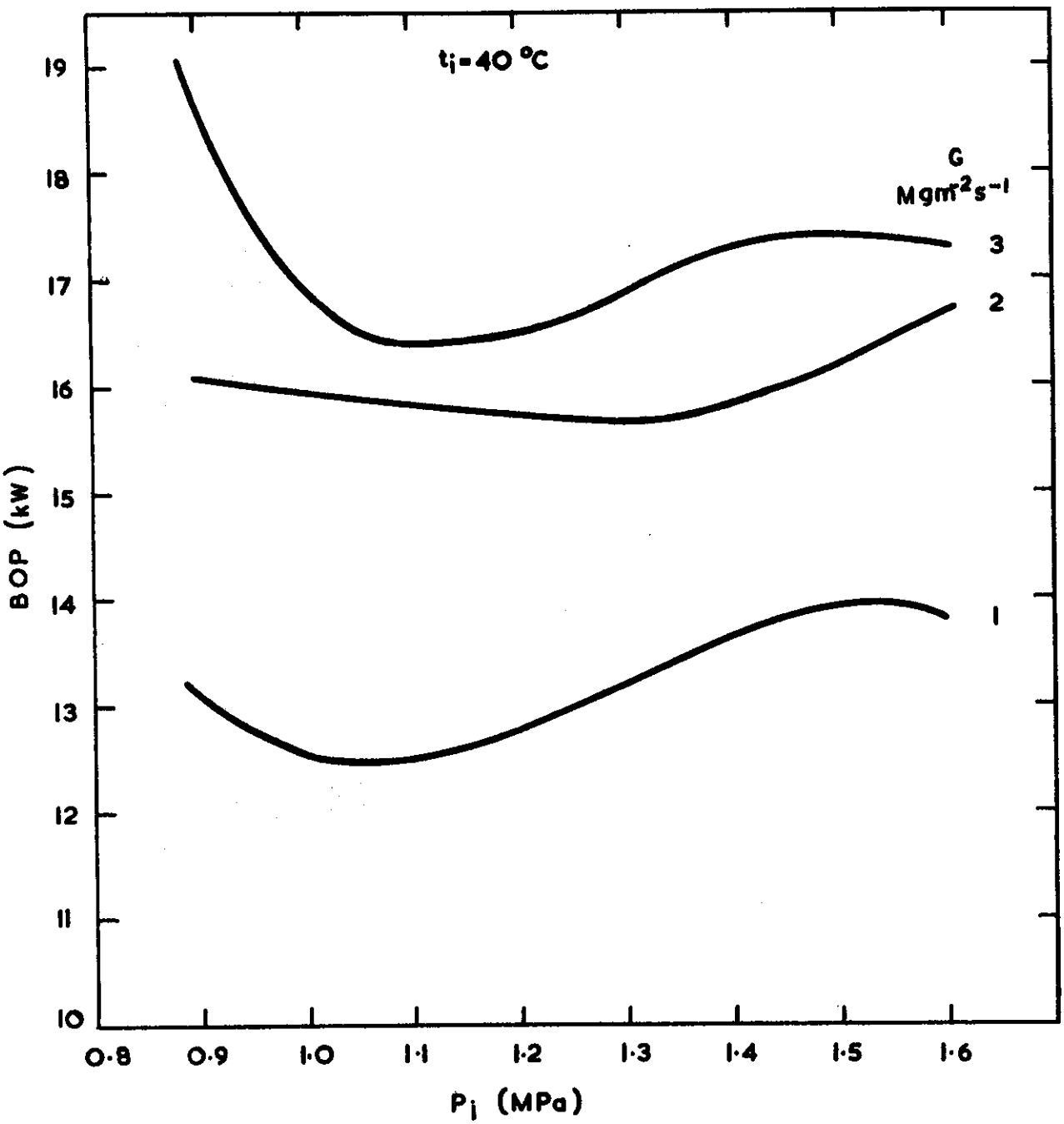

FIGURE 3. VARIATION OF BOP WITH p_i AT 40°C INLET TEMPERATURE FOR MASS VELOCITIES 1, 2 AND 3 Mg m^{-2}s^{-1}

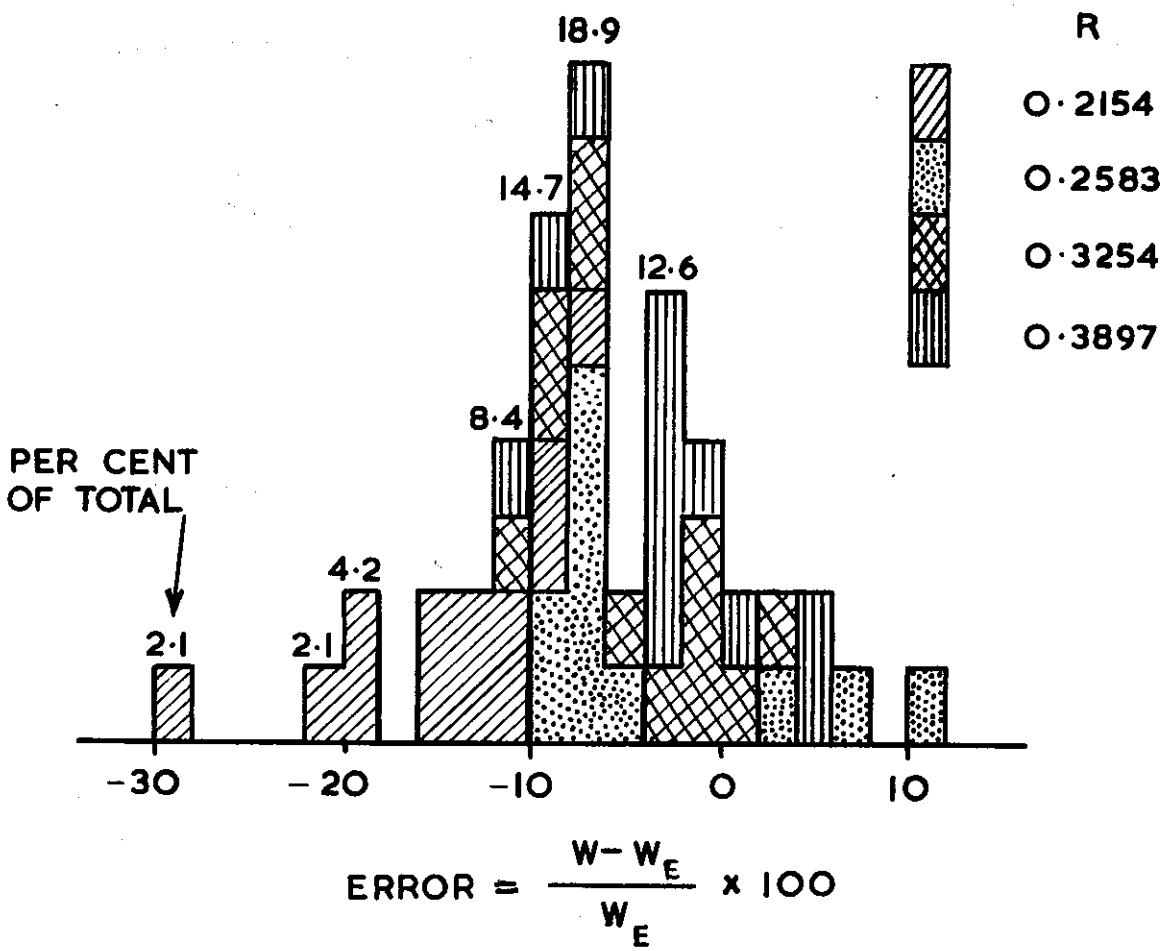

FIGURE 4. BOP CISE CORRELATION ERROR HISTOGRAM